Non-uniform temperature district heating system with decentralized heat storage units, a reliable solution for heat supply

Moallemi, Ali; Arabkoohsar, Ahmad; Pujatti, FJP ; Valle, Ramon Molina; Ismail, Kamal Abdel Radi

Published in:
Energy

DOI (link to publication from Publisher):
10.1016/j.energy.2018.10.188

Publication date:
2019

Document Version
Accepted author manuscript, peer reviewed version

Accepted Manuscript

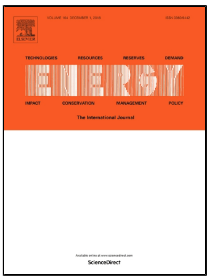

Non-uniform temperature district heating system with decentralized heat storage units, a reliable solution for heat supply

A. Moallemi, A. Arabkoohsar, F.J.P. Pujatti, R.M. Valle, K.A.R. Ismail

PII:	S0360-5442(18)32185-6
DOI:	10.1016/j.energy.2018.10.188
Reference:	EGY 14085
To appear in:	*Energy*
Received Date:	31 May 2018
Accepted Date:	29 October 2018

Please cite this article as: A. Moallemi, A. Arabkoohsar, F.J.P. Pujatti, R.M. Valle, K.A.R. Ismail, Non-uniform temperature district heating system with decentralized heat storage units, a reliable solution for heat supply, *Energy* (2018), doi: 10.1016/j.energy.2018.10.188

Non-uniform temperature district heating system with decentralized heat storage units, a reliable solution for heat supply

A. Moallemi[1], A. Arabkoohsar[2,*], F. J. P. Pujatti[1], R. M. Valle[1], K. A. R. Ismail[3]

[1]Department of Mechanical Engineering, Federal University of Minas Gerais, Belo Horizonte, Brazil

[2]Department of Energy Technology, Aalborg University, Denmark

[2]Faculty of Mechanical Engineering, State University of Campinas, Sao Paulo, Brazil

*Corresponding Author: ahm@et.aau.dk

Abstract

In this work, the novel concept of non-uniform temperature district heating system is proposed and analyzed. This system mainly works on a low-temperature supply mode for space heating, while it goes to high-temperature mode for domestic hot water supply only 4 hours a day. The system employs decentralized heat storage units to be charged during the high-temperature mode. In this way, the system operates based on a minimum rate of heat loss and there is no legionella risk due to thermal disinfection. The system is designed for a town in Brazil and a detailed thermodynamic model of the system is presented. The performance of this system is compared with other popular district heating schemes. With a total annual heat loss of 64 MWh, the proposed system outperforms the third generation technology in which the loss is almost double. As such, although the heat loss of the ultralow-temperature system is 28% lower (i.e. around 50 MWh), the non-uniform temperature system is still preferred to this case as well. This is because not only the proposed case supplies both of the hot water and space heating demands of the buildings, but also it does not need any further actions for legionella prevention.

Keywords: District heating system; Non-uniform supply temperature; Decentralized storage unit; Energy performance; Stratified storage tank.

1. Introduction

District heating is an important part of the future energy systems, so-called smart energy systems [1]. In the smart energy systems, there is a strong synergy between different energy systems/sectors so that the surplus energy in any sectors/systems can directly be utilized with others. Another main feature of the smart energy systems is the high integration of the renewable sources, where the district heating networks may facilitate the utilization of the low-grade renewable sources to a great extent [2].

Transition from the current state of the district heating technologies, i.e. the third generation (3GDH), to the next generation, so-called as the fourth generation (4GDH), is the cornerstone of a major part of the studies in this context [3]. The main futures of the 4GDH systems are the lower supply temperature, the big share of renewable energy, the two-way heat exchange with the end-users, the high integration of waste heat sources, etc. [4]. The first comprehensive report on the expected features of the 4GDH was given by Lund et al. [5]. Ziemele et al. [6] analyzed the transition of the Latvian district heating system to the fourth generation by considering various policies. Paiho and Reda [7] studied the smooth transformation of the Finnish district heating towards its fourth generation and discussed the challenges. Lund and Mohammadi [8] studied the insulation standards for a 4GDH system and proposed a combined heat loss and integrated energy system analysis method for the assessment of the insulation proficiency. Tereshchenko and Nord [9] studied the possible elements of the heat production chain in the future district heating systems considering various efficient energy conversion technologies, the economic aspects, and the technical limitations. Averfalk and Werner [10] highlighted the essential improvements in the future district heating systems, providing some recommendations on the design and construction strategies of the 4GDH. Kamal [11] accomplished a feasibility study for the methods of integrating the new coming 4GDH systems into the existing technology.

Apart from those studies investigating the transition to the 4GDH system, there are a large number of works that specifically study the possibility of decreasing the supply temperature, and consequently decreasing the rate of heat loss, in district heating systems. The concepts of low-temperature (LTDH) and ultralow-temperature (ULTDH) district heating systems as well as new substation designs are of the results of the efforts in this framework. In this regard, for instance, Olsen et al. [12] presented different recommendations for the district heating systems to enable the low temperature of 50 °C. Wang et al. [13] implemented a combination of high- and low-temperature district heating networks connected to an organic Rankine cycle for an energy efficient building. In this system, the organic Rankine cycle generates electricity using high-temperature district heat and the excess low-temperature heat is used to heat the building. Ancona et al. [14] presented several different layouts for the utility substations in the LTDH systems. Yang et al. [15] carried out a thorough energy, economy and exergy evaluation of the solutions for supplying domestic hot water (DHW) from an LTDH system with the supply temperatures of 65 ^{o}C, 50 ^{o}C, and 35 ^{o}C. Ommen et al. [16] investigated the optimal integration of booster heat pumps

in a ULTDH system. Yang and Svendsen [17] analyzed the return temperatures of different types of substations in a ULTDH system with a supply temperature in the range of 35-45 ^{o}C, and developed improvements in the substation designs for better energy efficiency. Chiu et al. [18] investigated the use of mobile thermal energy storage with phase change materials for utilizing industrial surplus heat flows for an LTDH network.

In this work, the new concept of non-uniform temperature district heating (NUTDH) system is proposed. This system works based on the predominant supply temperature of 40-45 ^{o}C (for 20 hours a day) and the periodic high temperature of 70-75 ^{o}C (for four hours a day). In the NUTDH system, the low-temperature supply is mainly for space heating, and the high-temperature supply aims at providing the DHW of the network. Since the high-temperature supply is not available all the time, the network is equipped with decentralized heat storage units to be charged during the high-temperature supply mode and be discharged during the regular operation of the system. To assess the performance of this system, it is designed and simulated for a small town in the southern part of Brazil. The system is analyzed for an entire year of operation. In addition, in order to evaluate the system performance compared to the other district heating schemes, the most popular district heating schemes of today, i.e. the 3GDH and the ULTDH systems, are also designed and thermodynamically analyzed for the case study. In the end, the obtained results are compared and discussed.

2. The NUTDH, the 3GDH, and the ULTDH Systems

In this section, first, the main characteristics of the 3GDH and the ULTDH systems are discussed, and then, detailed information about the NUTDH system is presented. The main reason for assessing the 3GDH and ULTDH schemes in this work is to address their weak points and explain why these technologies do not comply with the 4GDH system standards and also, to show how the NUTDH system properly addresses these drawbacks.

2.1. The 3GDH system

The 3GDH technology is, in fact, the currently in-operation district heating scheme in most of the world's energy systems. In this system, the design supply temperature is mainly in the range of 70-85 ^{o}C, while the design return temperature is in the range of 35-45 ^{o}C [19]. Apart from the dramatic change of heat production units, which is out of the scope of this work, the lower supply and return temperatures, the new generation of pipes, and the configuration of the substations are the main differences of the 3GDH system with the second generation of district heating systems [20]. Two substation designs are normally used in the 3GDH system. These substations are the instantaneous heat exchange unit (IHEU) and the district heating storage unit (DHSU). In an IHEU, the DHW section has just a plate heat exchanger, while in a DHSU, besides that, there is a buffer tank that stores heat for peak shaving. The

storage tank in the substation results in a significant reduction of the size of piping and heat exchangers, however, it causes a bigger rate of heat loss in the system [12]. The space heating section in both of these substations has only a plate heat exchanger. Fig. 1 shows the schematic of an IHEU (a) and a DHSU (b). The figure presents information about the temperature values before and after the substations based on the Brazilian comfort standards. T_A is the temperature of domestic cold water, which is equal to room temperature.

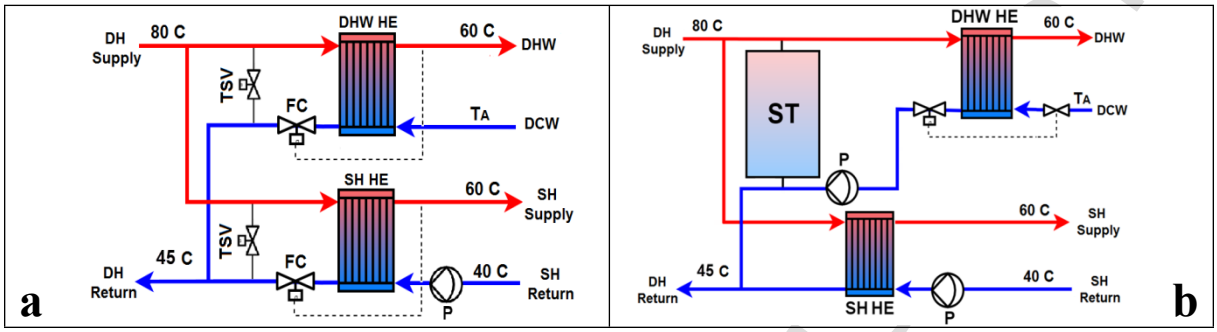

Fig. 1 Sketch diagram of the two main substation types in the 3GDH systems; the IHEU (a), the DHSU (b); DH: district heating, DHW: domestic hot water, DCW: domestic cold water, HE: heat exchanger, TSV: thermostatic valve, FC: flow controller, P: pump, SH: space heating.

2.2. The ULTDH system

The ULTDH system is similar to the 3GDH system in various aspects, e.g. the piping system, heat suppliers, etc. The only difference between these systems is the extremely lower temperatures of the ULTDH scheme, where the supply and return temperatures are in the range of 40-45 ^{o}C and 20-25 ^{o}C, respectively. Naturally, as the supply temperature is below the comfort standard of DHW, direct supply of hot water may not be possible. Therefore, either the ULTDH system is for space heating only (an auxiliary heater in the building covers the DHW demand) or the substation is equipped with a heat pump to increase the supply temperature to 60 ^{o}C. This substation design is called heat pump furnished unit (HPFU). Fig. 2 represents the schematics of a substation with an individual electrical heater (IEHU) (a), and an HPFU (b). As seen in Fig. 2-a, the hot water supplied by district heating is used for space heating only (via a plate heat exchanger) while in Fig. 2-b, in addition to space heating, the district heating water temperature is boosted to 60 ^{o}C by a heat pump for covering the DHW demand of the building. A thorough explanation of various HPFU designs may be found in [16].

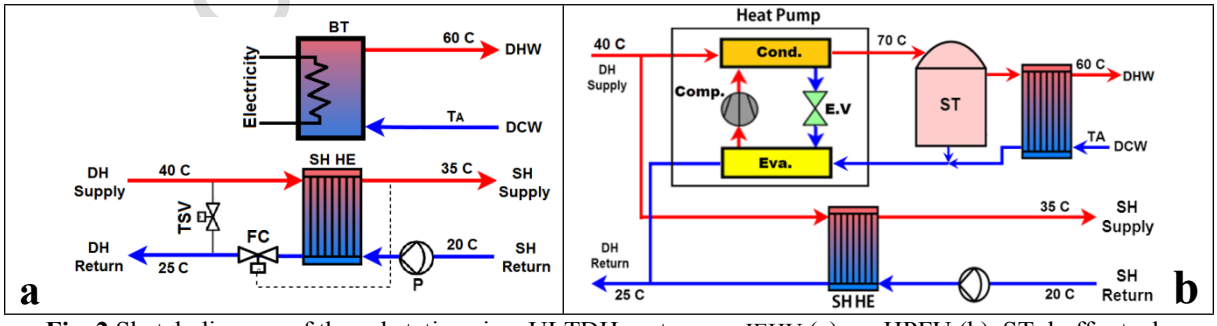

Fig. 2 Sketch diagram of the substations in a ULTDH system; an IEHU (a), an HPFU (b), ST: buffer tank.

2.3. The NUTDH system

As explained, one of the focuses of the studies on district heating technologies is to reduce the rate of heat losses for which the primary measure is to decrease the supply temperature as much as possible. This, however, can be challenging due to the main reasons of (i) the comfort standard DHW temperature, and (ii) the risk of the legionella. The legionella problem appears as a concern when the water temperature is between 25-45 ^{o}C and the standing time is longer than 2 days [21]. Since there is an extensive literature about the legionella problem in heat distribution systems, no further information about this issue is presented here. The DHW standard temperature varies from one country to another. For Brazil, the standard comfort DHW temperature is 60 ^{o}C [22]. Also, the standard comfort room temperature in residential buildings must be set at 26°C during summer and at 22°C during winter [23].

The NUTDH system aims at providing the DHW demand of the network at the standard comfort temperature and preventing the legionella risk, while a very low rate of loss is achieved. In fact, in the NUTDH system, the space heating demand is supplied by the low temperature of about 40-45 ^{o}C, while the high-temperature of around 70-75 ^{o}C is applied for a short period during the day for DHW preparation. The design low and high supply temperatures are chosen based on the comfort standard temperatures, the temperature drop along the pipeline and the expected efficiency of the heat exchangers.

As the NUTDH system is shortly on the high-temperature mode, the system needs heat storage units to be able to provide hot water for all day long. This work proposes the use of neighborhood-scale heat storage units. Fig. 3 presents the schematic diagram of the NUTDH system.

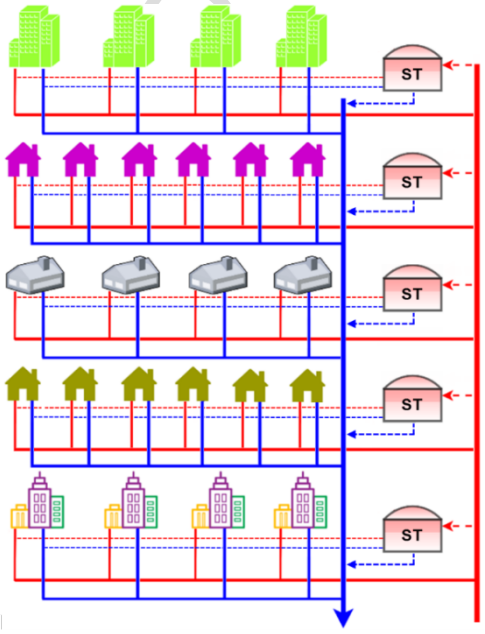

Fig. 3 Schematic of an NUTDH system; ST: storage tank, red: supply line, blue: return line, solid-lines: flows directly from/into the district heating system, dashed-lines: flows from/into the storage tank.

According to the figure, the main district heating lines bring the heat to the neighborhood (the streets

here) and the street branch pipes distribute the heat along each neighborhood. There is a further street connection line for connecting the storage tanks to the end-users. This supply/return twin pipe is much smaller than the main street connection pipe because not only it just provides the DHW demand, but also the simultaneity factor is quite low (due to the large number of houses in each neighborhood).

A further important point about this design is the way that the storage tanks are charged and discharged. As the storage tanks are to store district heating water, buffer tanks can be employed. Heat storage buffer tanks are stratified in various temperature levels (low temperatures below and higher temperatures above). The tank receives hot water from the top and the cold water goes out (to the return line) from the lower part of the tank. As the tank is charged, the temperature of the bottom of the tank also increases. If the control system does not work efficiently, the storage tank may discharge a considerable amount of heat back to the return line, causing a high rate of loss. For solving this problem, the storage tank employs a control valve that operates as a linear function of the temperature difference between the tank inlet and outlet flows, such that the lower the temperature difference gets (i.e. higher temperature of the bottom of the tank), the less the valve opens. Fig. 4 shows the storage tank configuration (a), and the control valve operating curve (b). In this figure, CV-1 is the electrical flow control valve for controlling the charging process, and CV-2 is the control valve that opens as much as the neighborhood demands. As seen in Fig. 4-b, the maximum temperature difference is 30 ^{o}C. As the temperature difference gets lower, the valve proportionally closes. The valve will be fully open for the higher temperature difference values than 30 ^{o}C.

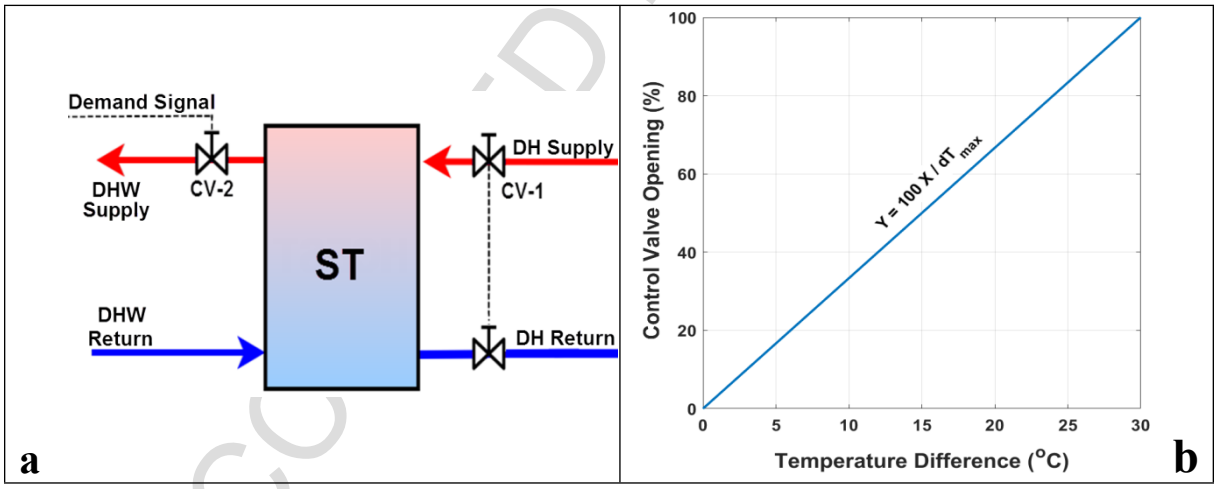

Fig. 4 storage tank operation/control strategy; the tank configuration (a), the control valve opening strategy (b), CV: control valve.

Finally, Fig. 5 shows the operation strategy of the NUTDH system for a sample three-tank network when working in high-temperature mode (a) and low-temperature mode (b).

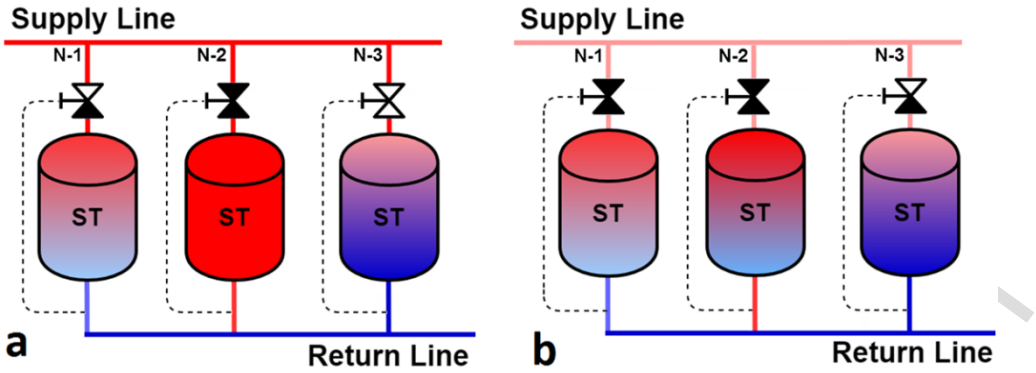

Fig. 5 Sketch of the NUTDH system operation strategy; high-temperature supply mode (a), low-temperature supply mode (b), N: neighborhood number; black valve: fully closed, white valve: fully open, black-white valve: partially open.

According to Fig. 5-a, if the system is in the high-temperature mode, the supply line charges all the tanks until they are fully charged. This figure shows that the storage tank of the second neighborhood is fully charged and as a result, its control valve is fully closed. In this case, neighborhoods 1 and 3 are being charged yet. As the temperature of the third tank is lower than the first one, its control valve opens more than the other one. Fig. 5-b shows the operating strategy of the system when the district heating system is on the low-temperature mode. In this case, the storage tanks are only charged if they are sufficiently cold. In the illustrated case, it is only the control valve of the third tank which is partially open due to the too low temperature of this tank.

It should be noted that the district heating system could be off during most of the days in summer as there will not be any space heating demand and the system only comes into operation to charge the storage tanks during the high-temperature mode.

Table 1 presents information about the characteristics considered for the 3GDH, the ULTDH and the NUTDH systems in this work.

Table 1 The features considered for the three different district heating schemes of this work.

Parameter	Information		
	3GDH	ULTDH	NUTDH
Space heating temperatures (°C)	70/40	35/25	60/40 or 35/25
Design supply temperature (°C)	80	40	75/45
Design return temperature (°C)	45	25	35/25
Substation design (DHW/SH)	IHEU or DHSU/IHEU	IEHU or HPFU/IHEU	IHEU/IHEU
Nominal pressure (barg)	12		
Space heating system	Radiator		
Pipe type	Twin [27]		
Insulation class	Series II and series III [27]		
Min pressure difference at the substation (bar)	0.3		
Max volume of each pipe after the substation (lit)	3		
Maximum media speed (m/s)	2		
DHW supply temperature (°C)	60		
Room comfort temperature (°C)	22		

3. The case study

The small town of Urupema in the Santa Catarina state of Brazil, with the latitude of -28° and the longitude of -49.9°, is the case study of this work. This small municipality, as one of the coldest cities in Brazil, is located in the south region of the country [24]. The fairly cold climate along with the high share of renewable sources, such as solar thermal and electricity system, wind energy, etc., make this point an appropriate location to host the smart district heating system designs. A total of 100 detached houses in the medium-sized category (with 2-4 inhabitants) are considered to be covered by a district heating system.

Generally, it is very challenging to find a database of heat consumption, and this gets even more difficult when information by category of consumption, i.e. space heating and DHW use, is required. The heat databases include the hourly heat consumption information and need to be refined to estimate what portion of this is used for space heating and what portion of the DHW demand coverage. In addition, such databases present the aggregated data instead of an individual building consumption. Therefore, it is not possible to drive an exact heat consumption profile for the buildings of the network. That is why, in this work, the heat consumption profiles of the individual buildings are created by calculating their space heating demand and randomization of a standard DHW draw-off pattern. This will be discussed comprehensively in the results section. In order to simplify the topology of the case study, the network shown in Fig. 6 is considered to be supplied by district heating.

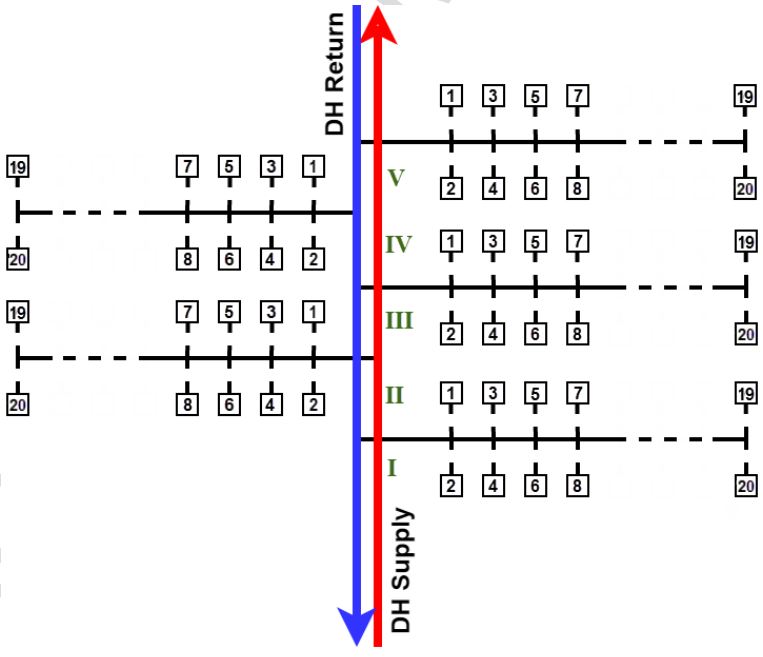

Fig. 6 Topology of the buildings in the network.

According to the figure, the network includes 5 streets, each with 20 detached-houses. The distance between the streets is 100 m, the distance of the houses in each street is 20 m and the houses are 10 m far from the street. The living area of each building is 150 m^2 on a 15 m × 10 m field.

4. Mathematical Model

In this section, the mathematical model of a district heating system is presented. For this, first, one should calculate the rate of heat loss and pressure drop along the pipeline. This would reveal at what temperature level the district heating water flow may reach the end-users, and how much work is required to drive the booster pumps for recovering the pressure drop along the way. Assuming a constant surface temperature for the pipe carrying the district heating water underground, Eq. 1 gives the temperature distribution profile of the water in the pipe [25]:

$$T(x) = \left(T_i - T_s\right) exp\left(\frac{UA_l x}{\dot{m}c}\right) + T_s \tag{1}$$

where, T is temperature, and the subscripts i and s refer to the pipe inlet condition and the soil surrounding the pipe. UA_l is the overall heat transfer coefficient from the water within the pipe to the soil, $\dot{m}$ is the mass flow rate, c is the thermal capacity of water, and x is the length of the pipe. Calculating the temperature distribution profile, one may calculate the rate of heat loss from x meter of the pipe by:

$$\dot{Q}_l(x) = UA_l(x)\left(T - T_s\right); \textbf{\textit{where}}: UA_l(x) = \left(\frac{1}{h_{in}\pi d_{in}x} + \frac{ln\left(\frac{r_{out}}{r_{in}}\right)}{2k_p\pi x} + \frac{ln\left(\frac{r_{ins,out}}{r_{ins.in}}\right)}{2k_{ins}\pi x}\right)^{-1} \tag{2}$$

where, r_{out}, r_{in}, $r_{ins,out}$ and $r_{ins,in}$ refer to the external and internal radiuses of the pipe and the insulation, respectively. k_p and k_{ins} are the conductivity factors of the pipe and the insulation material. h_{in} is the convective heat transfer coefficient. This parameter for a turbulent and a laminar flows through a pipe with a constant surface temperature may be, respectively, given by [25]:

$$h_{in-tur} = \frac{0.023 Re_D^{0.8} Pr^{0.4} k}{d_{in}} \tag{3}$$

$$h_{in-lam} = \frac{3.66k}{d_{in}} \tag{4}$$

where, Re_D is Reynolds number, Pr is Prandtl number, k is the conductivity of the fluid and d_{in} is the internal diameter of the pipe.

The rate of pressure drop through the pipe is given by:

$$\Delta P_t = \Delta P_f + \Delta P_{minor} = 1.2\ \Delta P_f; \textbf{ where: } \Delta P_f(x) = \frac{f x \rho u^2}{2d_{in}} \tag{5}$$

in which, ΔP_f and ΔP_{minor} are, respectively, the major pressure losses due to friction and the minor pressure losses through the pipe (approximately equal to 20% of the friction losses). ρ represents water density and u is the flow velocity. *f* is Darcy friction factor which is a function of the pipe roughness and Reynolds number as below:

$$f = \begin{cases} 0.316 Re_D^{-0.25} & if \quad Re_D \leq 20000 \\ 0.184 Re_D^{-0.2} & if \quad Re_D > 20000 \end{cases} \tag{6}$$

Having the value of the pressure losses, one may calculate the rate of work used by the booster pumps in the network as [26]:

$$\dot{W}_p(x) = \dot{m} v \Delta P_t = \frac{0.6 f \dot{m} x u^2}{d_{in}} \tag{7}$$

where, *v* is the specific volume of water.

The next step is modeling of the storage tanks. Practically, a storage tank may operate with significant degrees of stratification, i.e. the top of the tank hotter than the bottom. In a multi-node tank simulation approach, a tank is modeled as divided into N nodes (sections), with energy balances written for each of the nodes. The result is a set of N differential equations that can be solved for the temperature of the nodes as a function of time. Fig. 7 illustrates the arrangement of the nodes as well as the energy flows into/out of such a storage tank.

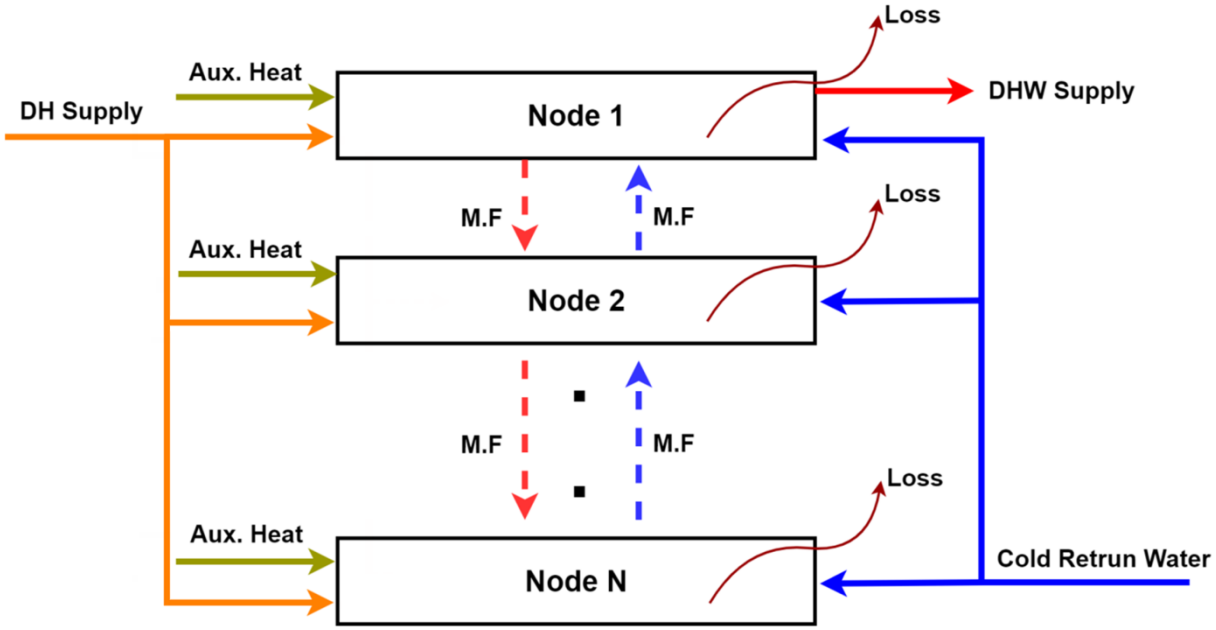

Fig. 7 Schematic of a multi-node heat storage tank; Aux. Heat: auxiliary heat source if any, M.F: mixing flows.

In this work, a five-node model is considered for modeling the neighborhood-scale storage tanks. For these tanks, the district heating water enters the tank from the top at the temperature of $T_{dh,s}$. The coming hot water flow lies in the first layer of the tank. Then, the same amount of water initially residing in the first node goes to the second node. Similarly, the water in each node moves to the lower node, and the same amount of water goes out to the district heating return line from the bottom node at $T_{dh,r}$. When discharging, the hot water supplied to the substations exits from the first node and it comes back to the tank through the bottom node. In addition to the energy transfer between the nodes due to mass transfer, the water layers exchange heat via thermal conduction due to the temperature differences.

Based on the first law of thermodynamics, the energy balance on each node of the tank can be written as follow [27]:

$$\underbrace{m_j c \frac{dT_{st,j}}{dt}}_{\dot{Q}_{std}} = \underbrace{F_j^{dh} \dot{m}_{dh} c (T_{dh,s} - T_{st,j})}_{\dot{Q}_{sp}} - \underbrace{UA_{l,j}(T_{st,j} - T_a)}_{\dot{Q}_l} - \underbrace{F_j^{dhw} \dot{m}_{dhw} c (T_{st,j} - T_{dhw,r})}_{\dot{Q}_{ld}} + \underbrace{kA_j \frac{(T_{st,j-1} + T_{st,j+1} - 2T_{st,j})}{y_j}}_{\dot{Q}_{ex}} + \underbrace{\begin{cases} \dot{m}_{mix,j} c (T_{st,j-1} - T_{st,j}) & if \quad \dot{m}_{mix,j} > 0 \\ \dot{m}_{mix,j} c (T_{st,j} - T_{st,j+1}) & if \quad \dot{m}_{mix,j+1} < 0 \end{cases}}_{\dot{Q}_{mix}} \quad (8)$$

In this equation, the subscripts/superscripts j, dh, dhw, mix, st, l, s and r refer to the number of the node, district heating water flow, DHW flow, mixing flows between the nodes, the storage tank, heat losses, supply line and return line, respectively. Also, m, dt, A, y are, respectively, the mass of water in each node, the duration of each time step (10 s), the cross-section area of each node and the height of each node.

Besides, two important parameters in this equation are $F_j^{dh,s}$ and $F_j^{dhw,s}$. The value of these parameters is either 1 or 0. $F_j^{dh,s}$ indicates which node the district heating water lies into, and the $F_j^{dhw,s}$ reveals which node the DHW return flow resides in. During the high-temperature mode, according to the explanation given, $F_j^{dh,s}$ is equal to 1 for the first node and 0 for the other nodes, while $F_j^{dhw,s}$ should be 1 for the bottom node and 0 for the others. Overall, these two factors may be calculated by:

$$F_j^{dh} = \begin{cases} 1 & if \quad j = 1 \ \textbf{and} \ T_{dh,s} > T_{st,j} \\ 1 & if \quad T_{st,j+1} < T_{dh,s} < T_{st,j-1} \\ 0 & if \quad otherwise \end{cases} \quad (9)$$

$$F_{j}^{dhw} = \begin{cases} 1 & if \quad j = N \textbf{ and } T_{dhw,r} < T_{st,j} \\ 1 & if \quad T_{st,j+1} < T_{dhw,r} < T_{st,j-1} \\ 0 & if \quad otherwise \end{cases} \tag{10}$$

As marked in Eq. 8, each of the statements on the left and right sides of the equation represent an energy flow in the control volume. Here, $\dot{Q}_{std}$, $\dot{Q}_{sp}$, $\dot{Q}_{l}$, $\dot{Q}_{ld}$, $\dot{Q}_{ex}$ and $\dot{Q}_{mix}$ refer to the rate of heat stored in each control volume, the injected heat into each node, the heat loss from each node, the heat load flow for DHW preparation, the heat exchanged between the nodes via conduction and the heat transferred among the nodes due to the mixing flows effect.

The above equation set can be solved by several numerical techniques such as the explicit Euler, the implicit Crank-Nicolson and Runge-Kutta methods. Fourth order Runge-Kutta method was employed in this work [28].

Regarding the substations, as discussed, each substation includes two plate heat exchangers. Considering counter-flow plate heat exchangers and an effectiveness factor of 0.8, the following equation series may be applied [29]:

$$\dot{Q}_{hx} = \dot{Q}_{dhw} \; or \; \dot{Q}_{sh} = UA_{hx}\Delta T_{lm} \tag{11}$$

where, Q_{hx} is the heat transferred from the district heating water to the secondary side of the heat exchanger, and should be equal to the DHW demand (Q_{dhw}) or space heating demand (Q_{sh}) of the buildings. UA_{hx} is the overall heat transfer coefficient of the heat exchanger and ΔT_{lm} is the logarithmic mean temperature difference. The temperatures of the hot and cold flows outgoing from each heat exchanger are calculated by:

$$T_{max,e} = \frac{\varepsilon_{hx} \overbrace{\dot{m}_{min} c_{min} (T_{max,i} - T_{min,i})}^{\dot{Q}_{max}}}{\dot{m}_{max} c_{max}} + T_{max,i} \tag{12}$$

$$T_{min,e} = T_{max,i}\varepsilon_{hx} + (1 - \varepsilon_{hx})T_{min,i} \tag{13}$$

in which, the subscript min refers to the fluid with the lower value of $C = \dot{m}c$ and the superscript max refers to the other fluid. In this equation, $\dot{Q}_{max}$ is the maximum possible heat transfer rate through the heat exchanger and ε_{hx} is the heat exchanger effectiveness factor given by:

$$\varepsilon_{hx} = \frac{UA_{hx}/C_{min}}{1 + UA_{hx}/C_{min}} \tag{14}$$

The heat demand in the DHW section depends on the hot water draw-off the building. This includes the small hand-washing tapings, the draw-offs for taking a shower, dishwashing, etc. and cannot be calculated or estimated. Instead, there are some standard taping profiles for families with different sizes that can be used as sample draw-off patterns. The energy demand for space heating, on the other hand, depends on the local standard comfort temperature, the ambient temperature, the building stuck energy performance, the performance of the heat distribution facilities and personal preferences. The following equation calculates the rate of demand for space heating:

$$\dot{Q}_{sh,b} = \underbrace{\rho_a V_{a,b}\left(T_{in}^{\,t+1} - T_{in}^{\,t}\right)}_{\dot{Q}_{s,b}} + \underbrace{\rho_a \dot{V}_{ven}\left(T_{in} - T_{out}\right) + UA_{l,b}\left(T_{in} - T_{out}\right)}_{\dot{Q}_{l,b}} + \underbrace{\rho_{bm} V_{bm}\left(T_{bm}^{\,t+1} - T_{bm}^{\,t}\right)}_{\dot{Q}_{std,b}} - \underbrace{\sum_{n=1}^{M}\left(A_n \mathrm{I_T}(\tau\alpha)_{avg}\right)}_{\dot{Q}_{g,b}} \quad (15)$$

in which, the subscripts a, in, out, b and bm refer, respectively, to the air within the building, the indoor condition, the ambient condition, the building and the building stuck material. The superscript t is the time step counter (in seconds), and V represents the volume. As marked, each of the statements on the right side of the equation represents an energy flow coming in or going out of the building. The first term on the right is the rate of heat required to increase the indoor temperature. The summation of the second and the third terms calculate the total rate of heat losses from the building via ventilation and heat loss to the ambient. In these two terms, $\dot{\mathrm{V}}_{\mathrm{ven}}$ is the volume flow rate of air replaced by fresh air for ventilation, and $\mathrm{UA}_{\mathrm{l,b}}$ is the overall heat loss coefficient of the building through the walls and windows. The fourth term indicates the rate of energy stored in the building stuck which will be zero in steady state conditions, and the last item calculates the rate of heat gain of the building due to solar irradiation. In this item, $\mathrm{I_T}$ is the solar irradiation through the windows, $\mathrm{A_n}$ is the area of each of the windows and $(\tau\alpha)_{\mathrm{avg}}$ refers to the average transmission-absorption coefficient of the windows and the internal elements of the building exposed to the sun rays. M is the total number of apertures letting sun rays coming into the building.

Calculating the energy demand of the network and the temperature drop through the pipe, one could size the pipeline of the district heating system. This includes dimensioning of the main distribution pipes, the street branches and house-connection pipes. For this, information about the supply and return temperatures are required. Naturally, the pipeline is such sized that it may carry the maximum heat load of the network based on the maximum allowed velocity through the pipes, i.e. 2 m/s. The following equation is used for sizing the pipeline:

$$d_{n,p} = \left(\frac{4\dot{Q}_{max}}{\rho\pi u_{max} c\Delta T}\right)^{0.5} \quad (16)$$

where, $d_{n,p}$ is the nominal diameter of each section of the pipeline, $\dot{Q}_{max}$ is the maximum heat load of the given pipeline section, u_{max} is the maximum velocity of water in the pipe, and ΔT is the temperature difference between the return and supply lines.

It bears mentioning that the simulation of the performance of the system via the above presented mathematical model is accomplished via programming in MATLAB.

5. Results and discussions

In this section, the results of the simulations on the NUTDH system and the other district heating schemes are presented. For this, first, one needs to create rational demand profiles for the network. For DHW draw-off profile, the following standard draw-off pattern (detailed in Table 2), which is recommended for a medium-sized family, is used. According to the table, there are several hand washing draw-offs (A) with a flow rate of 3 lit/min each, two shower draw-offs a day (B) with the flow rate of 6 lit/min each, and two further draw-offs with the flow rate of 4 lit/min (C and D).

Table 2 Standard DHW tapping pattern for a medium-sized dwelling.

Time	**min**	00	05	30	01	15	30	45	00	30	30	30	45	45	30	30	30	00	15	30	00	30	15	30
	hr	7	7	7	8	8	8	8	9	9	10	11	11	12	14	15	16	18	18	18	19	20	21	21
Draw-off Type		A	B	A	A	A	A	A	A	A	A	A	A	C	A	A	A	A	A	A	A	D	A	B
Information		A: 0.105 kWh; 3 lit/min C: 0.315 kWh; 4 lit/min														B: 1.4 kWh; 6 lit/min D: 0.735 kWh; 4 lit/min								

The total daily draw-off of this pattern is 100 lit for each building. As this profile seems lighter than real-life water tapping, a correction factor of 25% is used to weight up the loads in each category. For making the DHW profile of the whole network, this profile is randomized for all of the buildings. This is simply done in MATLAB. Fig. 8 shows the resultant DHW demand of the whole network over a sample day. In practice, a larger draw-off trend should be observed during early-morning and early-evening hours. Although this trend is not observed in the figure, the logical total daily tapping value and the fluctuating trend of the profile make the pattern an appropriate reference for the simulations.

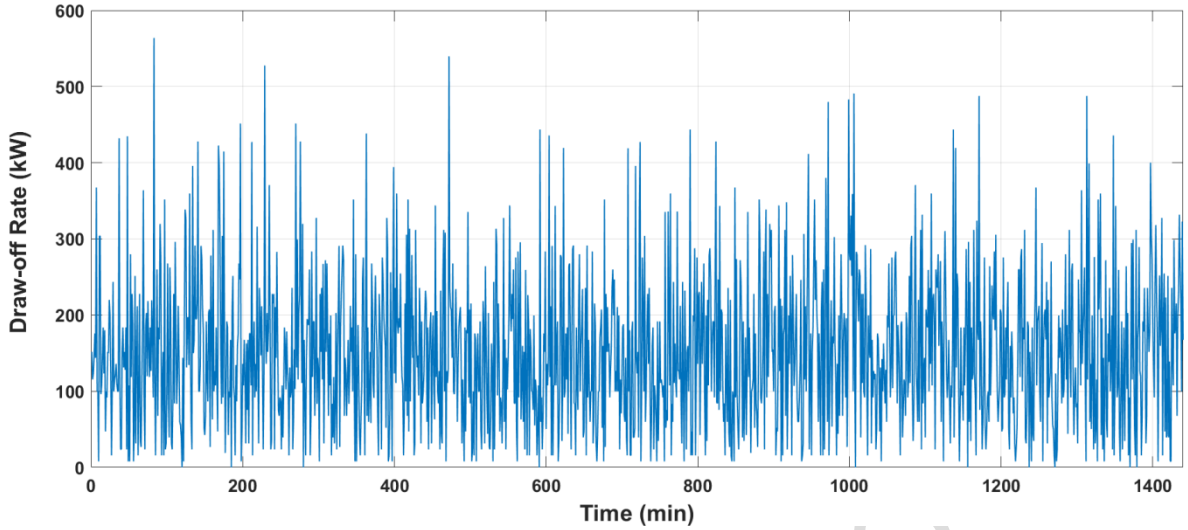

Fig. 8 DHW draw-off profile of the entire network during a day.

The space heating demand of the network is calculated by considering several factors, such as the ambient temperature, the standard comfort temperature, the buildings stuck thermal performances, etc. Fig. 9 illustrates the ambient temperature of Urupema in a monthly averaged format over the entire year 2015 [30].

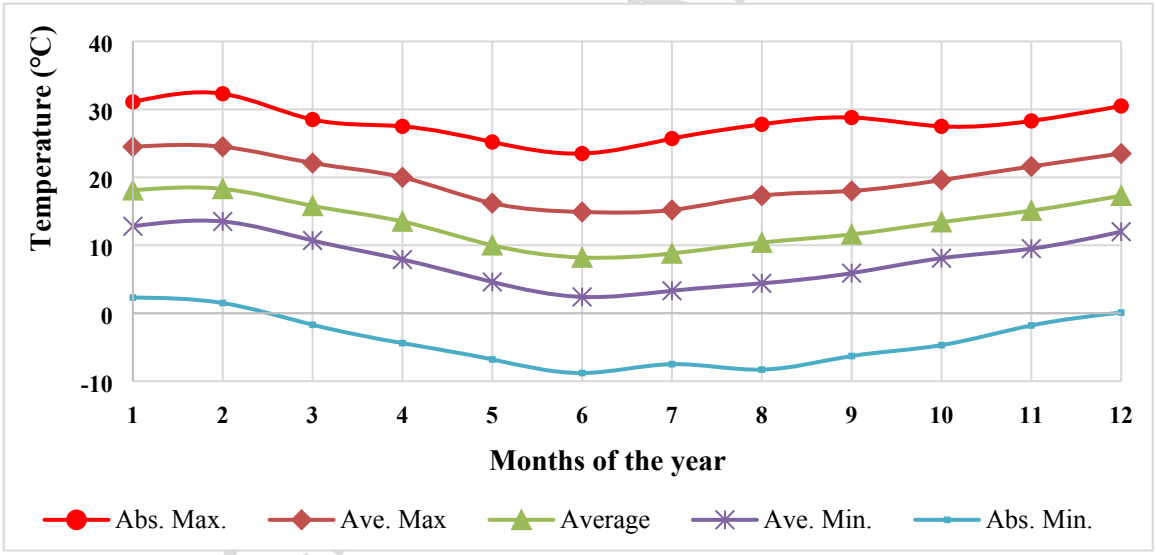

Fig. 9 Information about the ambient temperature of Urupema city in 2015.

As an important factor on the space heating demand of the network, the solar irradiation in this area is also needed. Fig. 10 presents information about the minutely measured solar irradiation on a horizontal surface with 1 m^2 area in Urupema during 2015 [30].

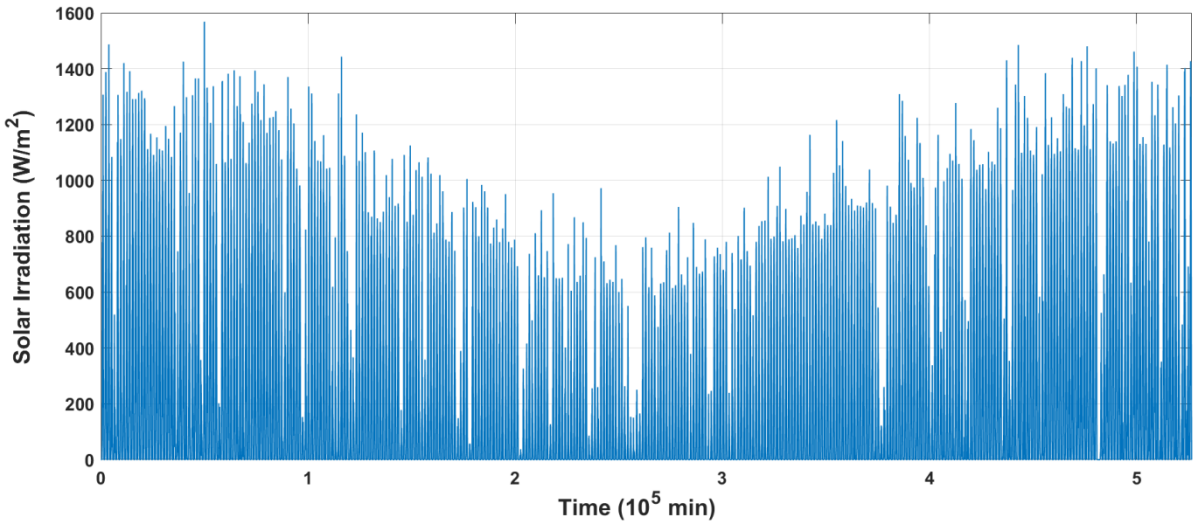

Fig. 10 solar irradiation availability in the case study during 2015.

For the buildings of the network, according to [31], an average overall heat loss factor of 0.93 W/m².K is considered. This is based on 2.32 W/m².K for windows (20% of the building shell surface), 0.625 W/m².K for walls (30%), 0.5 W/m².K for roofs (25%) and 0.625 W/m².K for the floor including cold bridges (25%). As all the buildings in the network are considered to be residential, the average hourly air exchange rate for ventilation is 0.5 m³/h per m³ of the heated building volume. The average daily internal gain of the building due to the inhabitants' metabolism effects is 2.3 °C [31].

In Brazil, the standard NR 17-Ergonomics from 1990 defines the acceptable thermal comfort conditions by defining the limits of effective temperature between 20 and 23 °C, air velocity is set to be less than 0.75 m/s and humidity should be above 40% [32]. In this work, the desired indoor temperature is set on 22 °C. Having said all these, one may calculate the space heating demand of each of the buildings, and subsequently, the entire network. Fig. 11 presents information about the heating demand of each of the buildings over the year. Clearly, as the comfort temperature and the characteristics of the buildings are considered the same, similar heat demand profile is obtained for all of the end-users in the network.

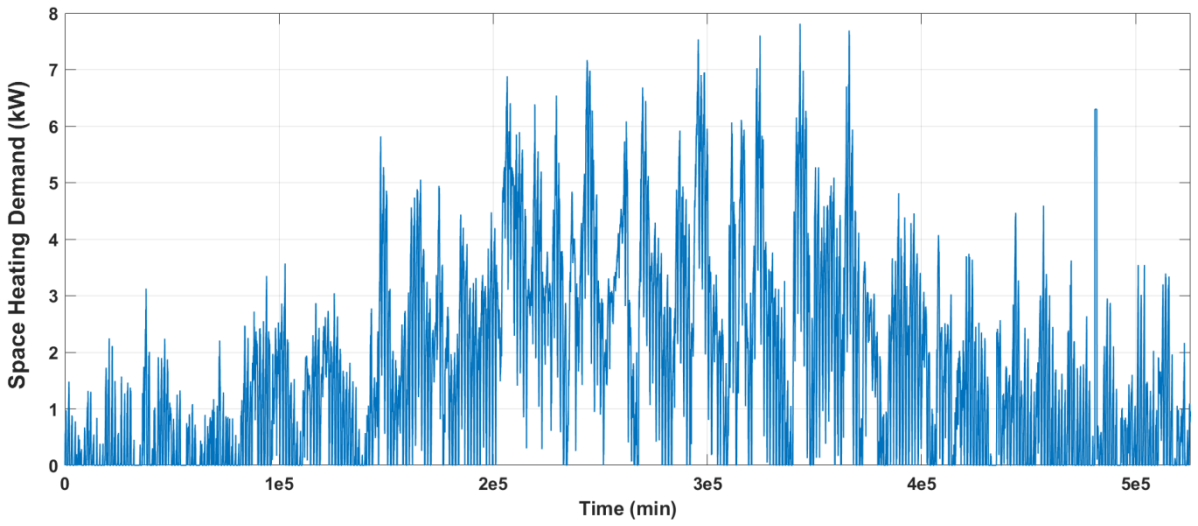

Fig. 11 Space heating demand of each building in the network over the year.

Having the randomized draw-off profile of the network and the space heating demand of the buildings, one may calculate the instantaneous total demand (space heating + hot water) of the entire network for each of the considered district heating schemes. Fig. 12 shows how different designs could result in the change of the district heating load. The figure is presented for three days of summer and three days in winter. The data is not presented for the entire year because this makes the graphs unreadable.

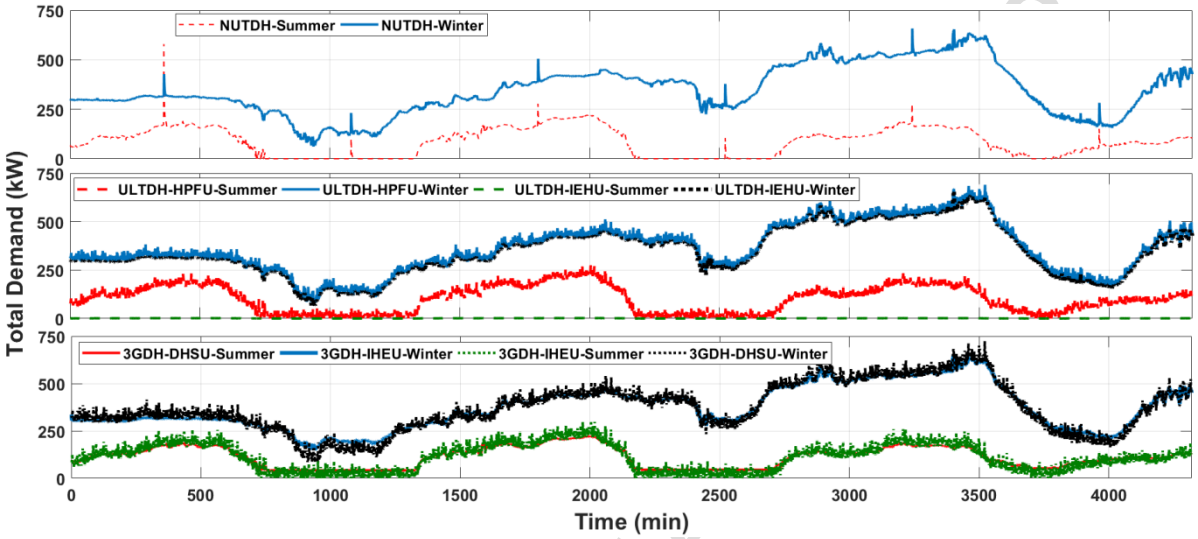

Fig. 12 The heat demand of various district heating systems for the case study over sample days.

According to the figure, the NUTDH system has a peak demand twice a day, i.e. when the heat storage units are charged. This decreases the load considerably during the rest of the day, even to a zero during the hot season. Between the two schemes of the ULTDH system, it is well observed how the IEHU would lead to a lower load because this system is for space heating only.

The main advantage of the heat pumps is enabling the ULTDH system to cover the DHW demand of the buildings, though it makes the substation be dependent on the electricity of the building and increases the cost of the substation dramatically. The heating duty of the ULTDH-HPFU system is calculated as:

$$\dot{Q}_{ult-hpf} = \dot{Q}_{sh} + \dot{Q}_{dhw}^{'}; \textbf{\textit{where}}: \dot{Q}_{dhw}^{'} = \dot{Q}_{dhw} - \dot{Q}_{cond-hp} \tag{17}$$

in which, $\dot{Q}_{ult-hpf}$ is the total heat load of a building when employing a ULTDH-HPFU scheme, $\dot{Q}_{dhw}^{'}$ is the share of the district heating system in DHW preparation of the building, $\dot{Q}_{cond-hp}$ is the heat provided via the condenser of the heat pump for DHW supply. The electricity required to derive the heat pump is calculated by:

$$\dot{E}_{hp} = \frac{\dot{Q}_{cond-hp}}{\beta_{hp}} = \frac{\dot{Q}_{dhw} - \dot{Q}_{dhw}^{'}}{\beta_{hp}} \tag{18}$$

where, β_{hp} is the coefficient of performance of the heat pump, assumed to be equal to 3 in this work.

Regarding the 3GDH scheme, it can be seen how employing a local storage tank can help for peak shaving in the network, decreasing the design capacity of the network. This peak shaving effect can be much more sensible if the draw-off is based on a large-scale family rather than the medium-sized families considered in this work.

Having the profiles of the instantaneous heat demands, and taking into account the design supply and return temperatures, one could see the differences between the flow rates of district heating water through the main distribution pipelines in each of the five different schemes. Fig. 13 gives information about this parameter. According to the figure, the flow rate in the 3GDH system is considerably lower than the other two designs. This is mainly because of the larger temperature difference between the supply and return lines in this scheme. In the ULTDH system, expectedly, the flow rate for the IEHU is smaller because it is only responsible for space heating.

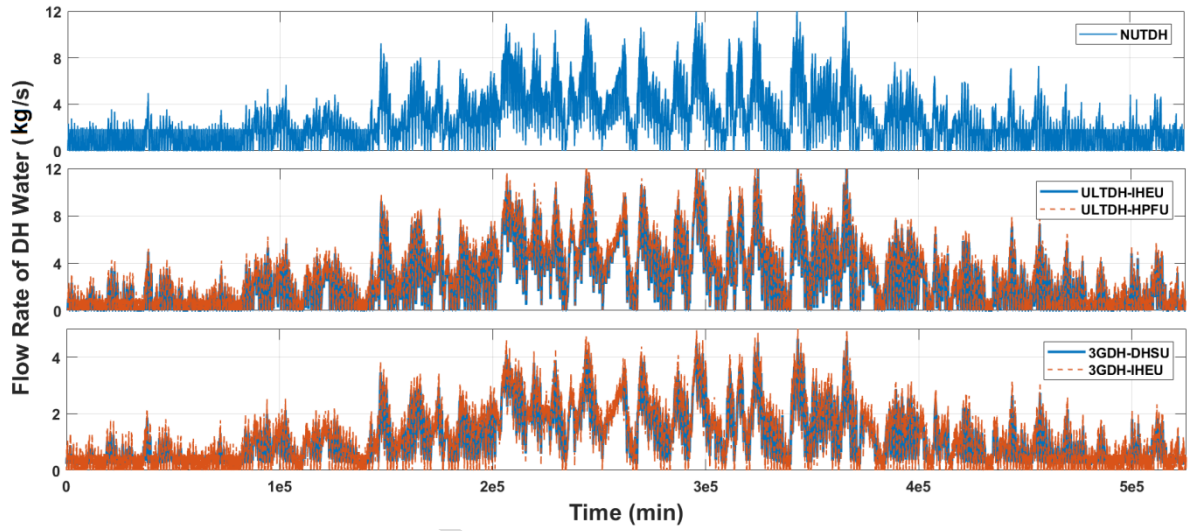

Fig. 13 Flow rate of district heating water through the pipeline of each of the considered cases.

Having the demands and flow rate profiles, the first step for analyzing the district heating systems is sizing the pipeline of each of the considered schemes. Table 3 presents detailed information about the size of pipes in various cases for the case study. It should be mentioned that for both of the 3GDH-DHSU and the ULTDH-HPFU systems small house connection pipes are obtained, however, these values are adjusted to 10 mm as the smallest possible house connection pipes. Note that the obtained dimensions for each of the systems may be different from the realistic systems and the main reason for this is the lack of realistic data for the DHW draw-off of the network.

Table 3. Size of the pipes for each of the considered systems.

	3GDH		ULTDH		NUTDH	
	DHSU	**IHEU**	**IEHU**	**HPFU**	**DHW Line**	**SH Line**
House Connection (Ø, mm)	10	11	10	15	10	10
Street Branch, 0-200 m (Ø, mm)	24	27	40	42	17	40

Street Branch, 201-400 m (Ø, mm)	17	21	28	31	14	28
Main Pipe, Part I (Ø, mm)	54	56	89	91	60	
Main Pipe, Part II (Ø, mm)	49	51	79	81	54	
Main Pipe, Part III (Ø, mm)	42	44	69	71	46	
Main Pipe, Part IV (Ø, mm)	34	37	56	58	38	
Main Pipe, Part V (Ø, mm)	24	26	40	41	27	

As seen, a 3GDH system with a DHSU substation configuration results in the smallest pipe dimensions. The main reason for this is the peak shaving that the storage tanks provide. On the other hand, the ULTDH system, with both substation types, requires the largest dimensions of the pipes. This is due to the small temperature difference of the district heating medium in the supply and return lines, i.e. only 15 °C. The NUTDH system needs the second largest pipes in the network because of the sharp sudden increase in the heat load of the system when the high-temperature supply starts. This can be modified through an optimization of the charging process of the heat storage units and the operation strategy of the flow control valves, which is the next part of this research project.

Having the dimensions of the pipelines and the flow rate of the water through the pipelines, one could make a comparison between the levels of pressure drop in each of the five scenarios. Naturally, when the pressure drop value is known, the amount of work required for the booster pumps to compensate the pressure losses may be calculated. Fig. 14 presents information about the instantaneous rate of pressure loss over the whole network for the various cases. The pressure drop profiles are only presented for 10 days in February as the hottest and 10 days of July as the coldest periods of the year. As seen, both of the 3GDH schemes show the lowest rates of pressure drop with a maximum rate of 1.7 MPa, because of the smaller flow rate of water through the pipeline. The NUTDH presents the highest rate of pressure drop with a peak value of 3.9 MPa.

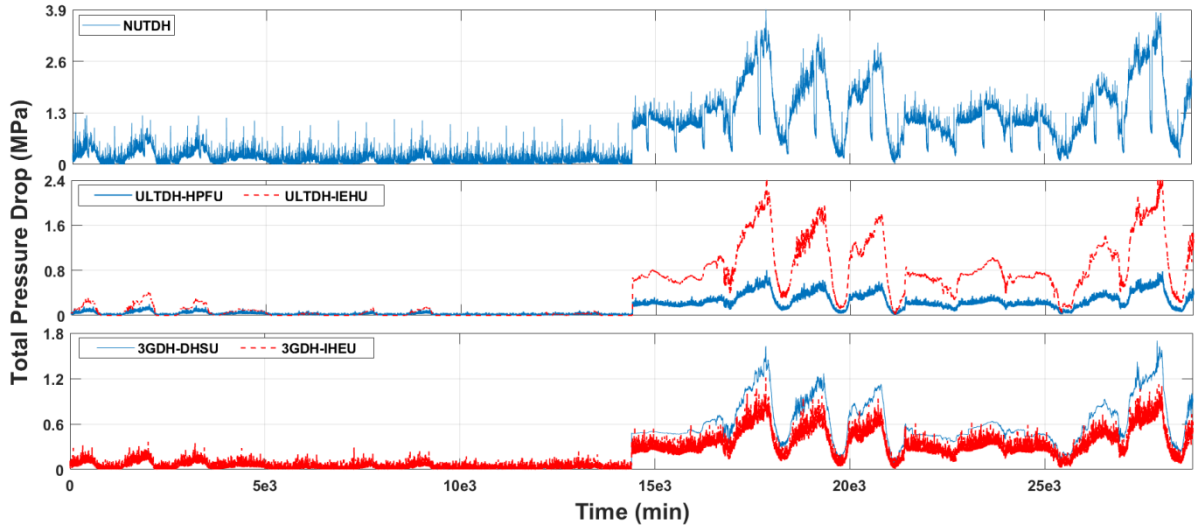

Fig. 14 Pressure loss rate in the entire pipeline for various cases.

Fig. 15 (a, b and c) shows the rate of heat losses in the five considered scenarios.

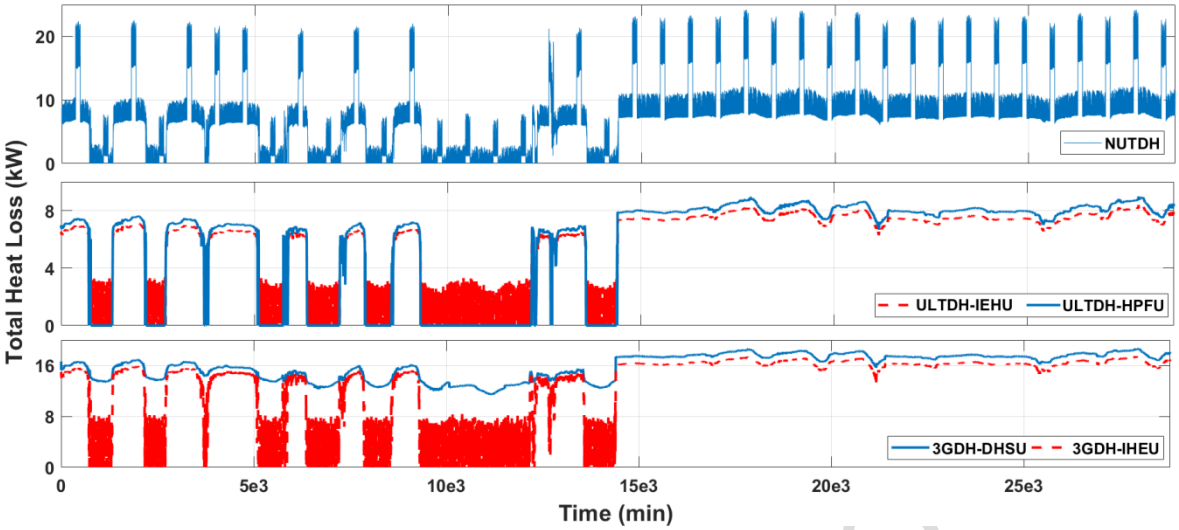

Fig. 15 The rate of heat losses in the entire pipeline of the considered scenarios for an entire year.

As seen, expectedly, both of the ULTDH systems show the best performances among the considered cases. This is mainly due to its ultralow temperature of supply along the pipeline all the time. Among these two, the system with the electrical heater performs insignificantly better because of the lower heating duty and consequently lower mass flow rate and smaller dimension of the pipes. It can be seen that the NUTDH system performs far better than both of the 3GDH schemes and its heat loss rate is not considerably higher than the ULTDH cases. Among the 3GDH systems that show the poorest performances among the five scenarios, the system with IHEU substation shows a better performance because of the heat losses from the storage tanks in each substation.

Considering the presented information about the performance of the various systems, Table 4 gives statistics about the total annual heat loss from the pipeline and the total annual pump work in each system. The table also presents the annual rate of heat loss, defined as the total annual amount of heat dissipated from the systems divided by that supplied to the network over the whole year. According to the table, and confirming the discussion above, it can be seen that the 3GDH-DHSU has the highest annual heat lost rate of 138.6 MWh and the low required pump work of 1.4 MWh. The 3GDH-IHEU system offers the lowest required amount of pump work with only 1.1 MWh while its annual heat loss is about the high value of 110 MWh. The high operating temperatures (that not only cause the highest rate of heat losses but also make the utilization of low-grade renewable energy and waste heat flows difficult) is the main reason why the 3GDH system is not compatible with the 4GDH system standards.

On the other hand, the ULTDH-IHEU and ULTDH-HPFU systems offer the lowest rate of losses of 45 MWh and 49.5 MWh, and the low pump works of 1.2 MWh and 1.4 MWh, respectively. A ULTDH system should definitely present the lowest rate of loss because of its ultralow-temperature all the time. As such, its low rate of pump work is because this system is in off during many periods of the year. Although the ULTDH system, in both substation types, presents the lowest rates of losses, this technology is not compatible with the 4GDH system requirements. The first reason for this is that it does

not provide the DHW of the end-users, and it needs an auxiliary heater for this purpose (i.e. the electrical heater and the heat pump). As seen in the last row of the table, the ULTDH schemes are the only technologies that do not cover all the heating demand of the network, i.e. 75% demand coverage by the IEHU and 83% coverage by the HPFU. The table shows that the ULTDH-IEHU and ULTDH-HPFU systems consume a total annual of 231.2 MWh and 77.1 MWh electricity in the buildings, respectively. This is in contrast with the main objective of district energy systems, i.e. to make the buildings independent of standalone energy systems. In addition, the previous studies show that the ULTDH-HPFU system does not offer a good cost-effectiveness, mainly due to the high cost of the heat pump in the substation [33]. Besides, the ULTDH systems require additional legionella prevention/elimination processes as the temperature range of 25-45 ^{o}C is the most appropriate condition for legionella growth and multiplication.

Finally, according to the table, the NUTDH system offers the highest pump work of 6.9 MWh for a year. This is not considered as a drawback as long as this system can provide the very low rate of heat loss of 64.2 MWh, which is almost half the 3GDH systems losses. This is equal to the interesting annual heat loss rate of 3.6%. Note that these values are much smaller than real life district heating systems where, for example, a regular 3GDH presents about 25-30% of heat loss. This is because, in this work, the heat loss from the distribution pipes is not taken into account by considering the heat production chain just near to the network. For the transmission losses of different cases, the given loss rate values could be simply scaled with the same ratios to each other.

Considering the presented results, one may conclude that the proposed NUTDH system may be an appropriate solution for the 4GDH system. This can be concluded because:

(i) it offers a very low rate of loss,
(ii) its very low average supply temperature facilitates the utilization of low-grade renewable technologies and waste heat flows.
(iii) the risk of legionella is totally solved via the periodic thermal disinfections (high-temperature operations).

Table 4 The details of the overall performance of various district heating cases in an entire year.

DH Scheme	**3GDH**		**ULTDH**		**NUTDH**
Substation Configuration	**IHEU**	**DHSU**	**IEHU**	**HPFU**	
Total Annual Work of Pump (MWh)	1.1	1.4	1.2	1.4	6.9
Total Annual Heat Lost (MWh)	109.2	138.6	45.0	49.5	64.2
Rate of Heat Loss (%)	6.2	7.8	2.8	2.9	3.6
In-Building Electricity Use (MWh)	0	0	231.2	77.1	0
Rate of Demand Coverage (%)	100	100	75	83	100

Hereafter, some of the key factors in the design and dimensioning of the NUTDH system are discussed. One of the key parameters in designing the NUTDH system for the case study is the size of the storage tanks for each neighborhood/street. Naturally, the larger the storage tanks are, the slower they are

discharged. Meanwhile, a larger storage tank has a higher cost and a larger rate of loss. Technically, based on the Brazilian DHW standard, the minimum top-node temperature of the storage tank should be 60 °C. Considering the effectiveness factor of the heat exchangers, the storage tank volume that provides the minimum top-node temperature of 65 °C during the year is opted as the optimal tank volume in this work. Fig. 16 shows the minimum top-node temperature observed among all the storage tanks in the network for various volumes. According to the table, a heat storage unit with 0.61 m^3 is the best choice for this system.

Fig. 17 shows the supply temperature of the storage tanks in the network over the two-hour charging periods in two typical seasonal days, i.e. one in summer and another in winter. This is an index of showing how the temperature drops along the pipeline. As seen, the level of temperature drop is larger for the further storage tanks because of the longer distance that the fluid passes and due to the reduction of the mass flow rate after each street, which increases the rate of heat losses. In addition, it is observed that the temperature drop during the summer day is larger. This is reasonable because the mass flow rate through the pipes is smaller in the summer and this causes a larger temperature drop along the pipe. Overall, the level of temperature drop is not significant due to the small length of the pipeline.

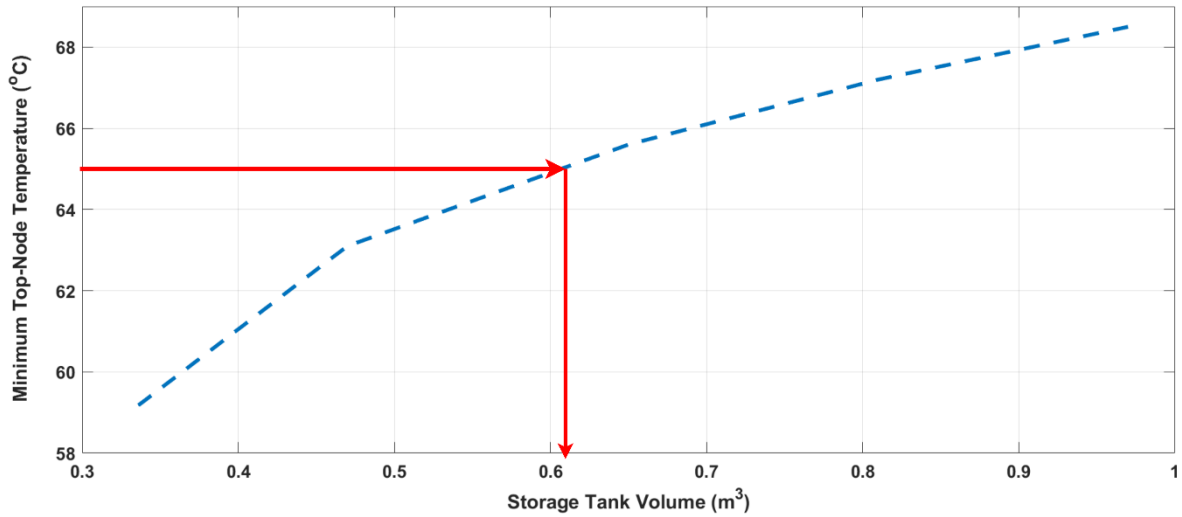

Fig. 16 Dimensioning the storage tanks in the NUTDH system.

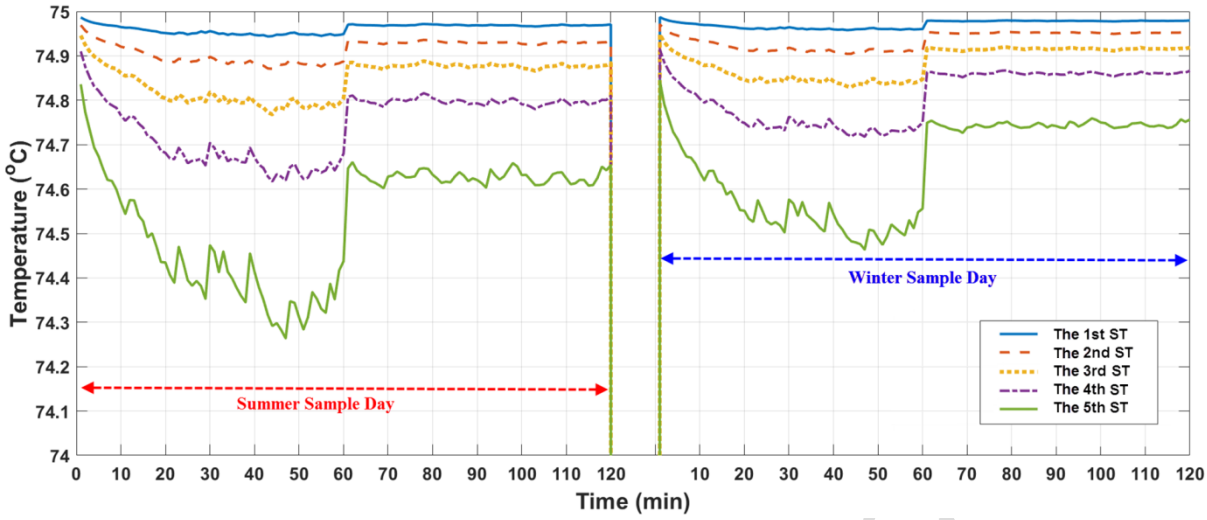

Fig. 17 Supply temperature of the storage tanks in two different sample days, ST: storage tank.

The next step is to present the results of the simulations accomplished on the heat storage tanks. Before that, one should validate the model and the numerical method used for this purpose. For this, the numerical results are compared with the experimental results reported in [34] for a storage tank with the height of 1.93 m, a diameter of 1.16 m, and an insulation thickness of 0.05 m. The tank is initially at the uniform temperature of 20.5 °C and is charged with a hot water flow at 39 °C and specific flow rates. The detailed characterisics of the tank and the experiment conditions are given in the reference work [34]. Fig. 18 makes a comparison of the numerical and experimental results for the given heat storage tank when hot water with a mass flow rate of 1364 kg/h is applied to charge the tank for 0.5 h, 1 h, and 1.5 h.

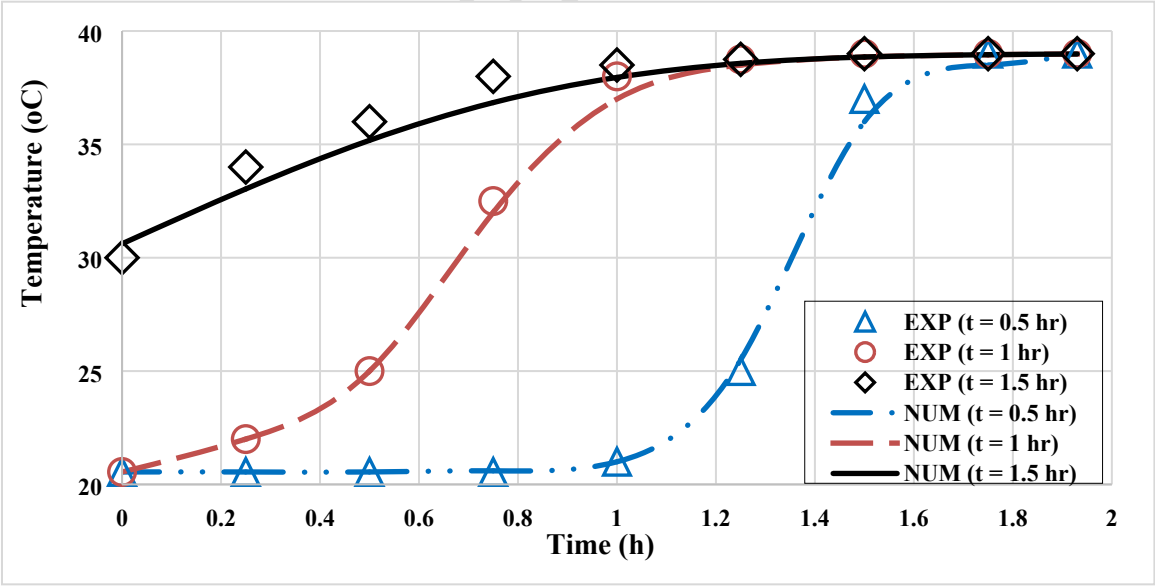

Fig. 18 Comparison of the numerical and experimental storage tank temperature distribution profiles.

As can be seen, there is a strong agreement between the layer temperatures predicted by the model and those reported by the experimental work. Therefore, the numerical model and method used for the stratified heat storage tanks can be reliably used in this work.

Fig. 19 shows the variation of the temperature of the storage tanks (at three levels of bottom, middle and top) over a sample winter day. This figure shows how the storage tank is charged during the charging time and how it is discharged when the system is in low-temperature mode. As the figure shows, all the nodes approach the supply high temperature during the charging phases. It is seen that the temperature profile of the bottom node of the tanks fluctuates more sharply. This is because the hot water of the upper nodes is replaced by the colder yet warm water of their below nodes, whereas for the bottom node, it is replaced by the cold water of the district heating return line (at 35 °C).

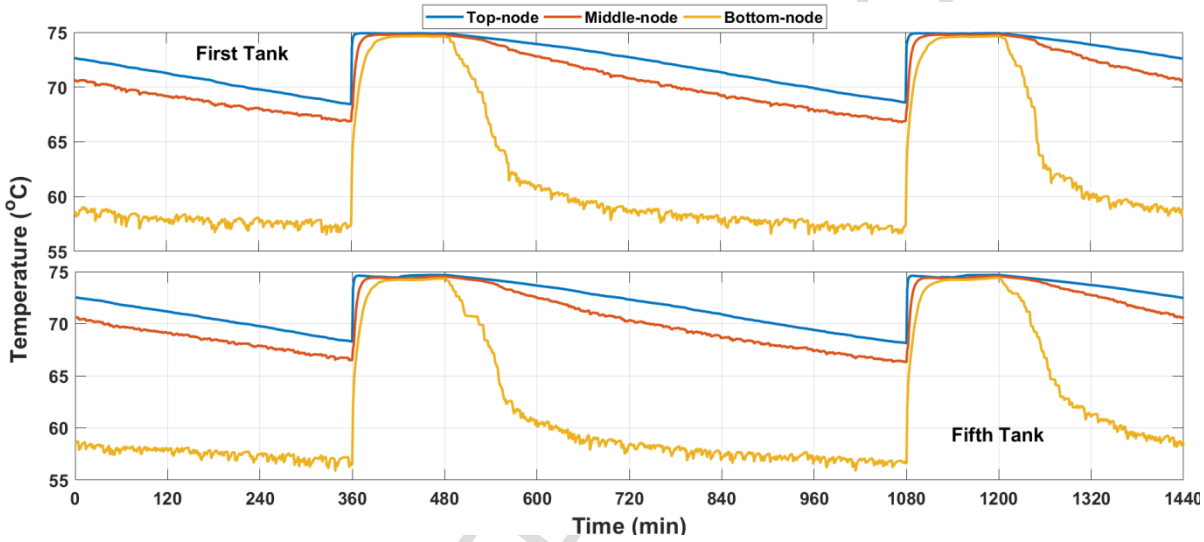

Fig. 19 Temperature of the tanks in different nodes over a sample winter day.

As discussed, the NUTDH system has two supply lines after the heat storage units, one for space heating and the other for supplying the DHW demand of the users. Fig. 20 and 21 compare the supply temperatures of a few buildings (building 1 in street I, building 10 in street III and building 20 in street V) in their DHW and space heating lines, respectively. These graphs are also presented for one winter day and one summer day. Note that, the DHW flow with a temperature higher than the standard value is mixed with cold water to reach the desired temperature level.

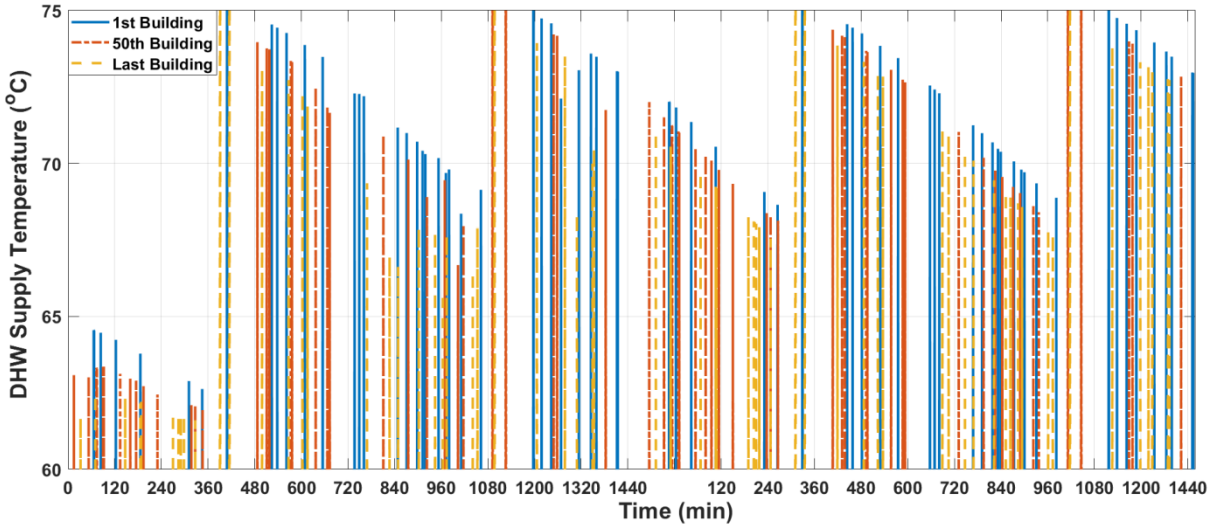

Fig. 20 DHW supply temperature of a few buildings in the network.

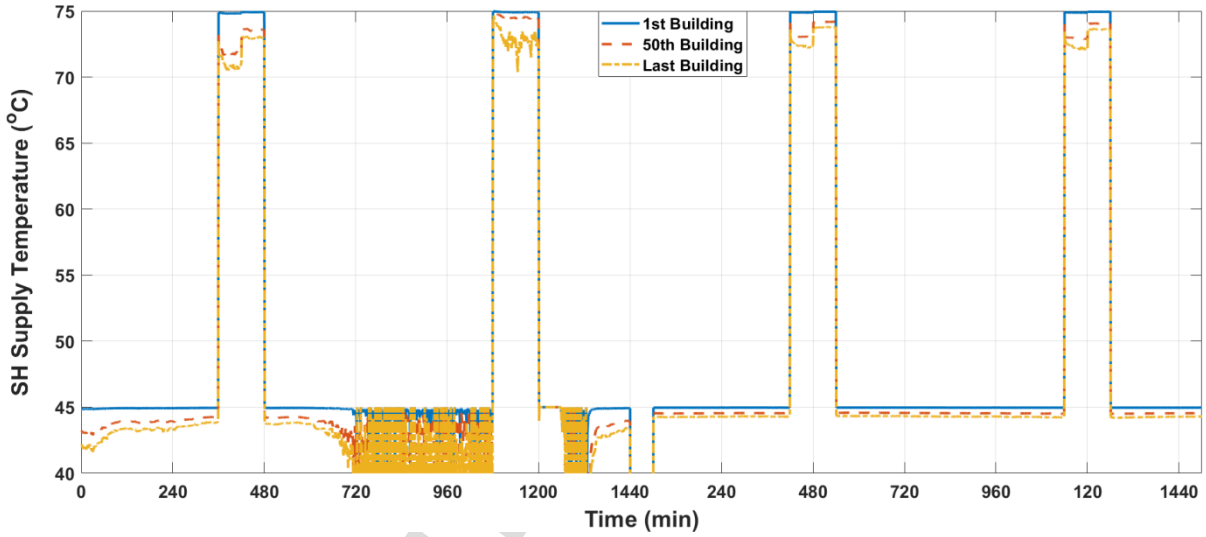

Fig. 21 Space heating supply temperature of a few buildings in the network.

6. Conclusion

In this work, the novel concept of NUTDH system was proposed and thermodynamically analyzed. The main objective of this work is to introduce the new heat supply technology that strongly meets the 4GDH systems' criteria, i.e. a very low heat loss rate; low supply/return temperatures so that low-grade renewable technologies and waste heat sources may integrate, etc. The system was precisely designed and sized in all the components and its performance was analyzed for a case study in Brazil. The results were compared with those obtained for the performance of other competitive district heating schemes, i.e. ULTDH and 3GDH systems with different substation configurations. The results showed that the system might sufficiently provide the required heat of the whole network for both space heating and DHW uses. It was proved that the NUTDH system, with a total annual loss of about 64 MWh, is

extremely more efficient than the 3GDH in both substation configurations with the annual heat losses of about 109 MWh and 138 MWh. The NUTDH loss is slightly higher than the ULTDH schemes with the annual heat losses of about 45 MWh and 50 MWh. Even though the loss of the proposed system is higher than the ULTDH schemes, it is still superior because not only the ULTDH schemes do not cover the DHW demand of the end-users and require in-building electricity supply, which is a serious drawback, but also they need additional legionella prevention measures. In addition, the ULTDH-HPFU system suffers from the too high cost of capital of the substation. Overall, the NUTDH system showed a high feasibility for being a dominant district heating scheme in the future, though it still needs more investigations in various techno-economic aspects to address the technical and practical gaps before being broadly implemented.

References

[1] H. Lund, P.A. Østergaard, D. Connolly, B.V. Mathiesen, Smart energy and smart energy systems, Energy. 137 (2017) 556–565. doi:10.1016/J.ENERGY.2017.05.123.

[2] H. Lund, N. Duic, P.A. Østergaard, B.V. Mathiesen, Smart energy systems and 4th generation district heating, Energy. 110 (2016) 1–4. doi:https://doi.org/10.1016/j.energy.2016.07.105.

[3] J. Ziemele, E. Cilinskis, D. Blumberga, Pathway and restriction in district heating systems development towards 4th generation district heating, Energy. 152 (2018) 108–118. doi:https://doi.org/10.1016/j.energy.2018.03.122.

[4] A. Volkova, V. Mašatin, A. Siirde, Methodology for evaluating the transition process dynamics towards 4th generation district heating networks, Energy. 150 (2018) 253–261. doi:https://doi.org/10.1016/j.energy.2018.02.123.

[5] H. Lund, S. Werner, R. Wiltshire, S. Svendsen, J.E. Thorsen, F. Hvelplund, B.V. Mathiesen, 4th Generation District Heating (4GDH): Integrating smart thermal grids into future sustainable energy systems, Energy. 68 (2014) 1–11. doi:https://doi.org/10.1016/j.energy.2014.02.089.

[6] J. Ziemele, A. Gravelsins, A. Blumberga, G. Vigants, D. Blumberga, System dynamics model analysis of pathway to 4th generation district heating in Latvia, Energy. 110 (2016) 85–94. doi:https://doi.org/10.1016/j.energy.2015.11.073.

[7] S. Paiho, F. Reda, Towards next generation district heating in Finland, Renew. Sustain. Energy Rev. 65 (2016) 915–924. doi:https://doi.org/10.1016/j.rser.2016.07.049.

[8] R. Lund, S. Mohammadi, Choice of insulation standard for pipe networks in 4th generation district heating systems, Appl. Therm. Eng. 98 (2016) 256–264. doi:https://doi.org/10.1016/j.applthermaleng.2015.12.015.

[9] T. Tereshchenko, N. Nord, Energy planning of district heating for future building stock based on renewable energies and increasing supply flexibility, Energy. 112 (2016) 1227–1244. doi:https://doi.org/10.1016/j.energy.2016.04.114.

[10] H. Averfalk, S. Werner, Essential improvements in future district heating systems, Energy Procedia. 116 (2017) 217–225. doi:https://doi.org/10.1016/j.egypro.2017.05.069.

[11] M. Kamal, POTENTIAL FOR LOW TEMPERATURE, (2017).

[12] J.-E.T. Peter Kaarup Olsen, Christian Holm Christiansen, Morten Hofmeister, Svend Svendsen, Guidelines for Low-Temperature District Heating, EUDP 2010-II Full-Scale Demonstr. Low-Temperature Dist. Heat. Exist. Build. (2014) 1–43.

[13] N.G. Hai WANG, Hai-ying WANG, Tong ZHU, Ed D, J. Zhejiang Univ. A (Applied Phys. Eng. 1775 (2010) 1–18. doi:10.1902/jop.2010.090575.

[14] M.A. Ancona, L. Branchini, A. De Pascale, F. Melino, Smart District Heating: Distributed Generation Systems' Effects on the Network, Energy Procedia. 75 (2015) 1208–1213. doi:https://doi.org/10.1016/j.egypro.2015.07.157.

[15] X. Yang, H. Li, S. Svendsen, Energy, economy and exergy evaluations of the solutions for supplying domestic hot water from low-temperature district heating in Denmark, Energy Convers. Manag. 122 (2016) 142–152. doi:https://doi.org/10.1016/j.enconman.2016.05.057.

[16] T. Ommen, J.E. Thorsen, W.B. Markussen, B. Elmegaard, Performance of ultra low temperature district heating systems with utility plant and booster heat pumps, Energy. 137 (2017) 544–555. doi:https://doi.org/10.1016/j.energy.2017.05.165.

[17] X. Yang, S. Svendsen, Achieving low return temperature for domestic hot water preparation by ultra-low-temperature district heating, Energy Procedia. 116 (2017) 426–437. doi:https://doi.org/10.1016/j.egypro.2017.05.090.

[18] J.N.W. Chiu, J. Castro Flores, V. Martin, B. Lacarrière, Industrial surplus heat transportation for use in district heating, Energy. 110 (2016) 139–147. doi:https://doi.org/10.1016/j.energy.2016.05.003.

[19] A. Arabkoohsar, G.B. Andresen, Supporting district heating and cooling networks with a bifunctional solar assisted absorption chiller, Energy Convers. Manag. 148 (2017) 184–196. doi:https://doi.org/10.1016/j.enconman.2017.06.004.

[20] Logstor, DH Pipeline Developer, (n.d.).

[21] J.E. McDade, *Legionella* and the Prevention of Legionellosis, Emerg. Infect. Dis. 14 (2008) 1006a–1006. doi:10.3201/eid1406.080345.

[22] O. Gerin, B. Bleys, K. De Cuyper, Domestic hot water consumption in apartment buildings, Symp. 2015. (2015). https://www.wtcb.be/homepage/download.cfm?dtype=research&doc=domestic_hot_water_flow_measurements_in_apartment_buildings.pdf&lang=en.

[23] R. Oliveira, R. Souza, M. Rizzi, A.J. Mairink, R. Silva, Thermal Comfort for Users According to the Brazilian Housing Buildings Performance Standards, 2015. doi:10.1016/j.egypro.2015.11.668.

[24] Portal do IBGE - Brazilian Institute of Geography and Statistics, (n.d.). https://www.ibge.gov.br.

[25] F.P. Incropera, T.L. Bergman, A.S. Lavine, D.P. DeWitt, Fundamentals of Heat and Mass Transfer, 2011. doi:10.1073/pnas.0703993104.

[26] J.P. Stark, Fundamentals of classical thermodynamics (Van Wylen, Gordon J.; Sonntag, Richard E.), J. Chem. Educ. 43 (1966) A472. doi:10.1021/ed043pA472.1.

[27] A. Arabkoohsar, M. Farzaneh-Gord, R. Ghezelbash, R.N.N. Koury, Energy consumption pattern modification in greenhouses by a hybrid solar–geothermal heating system, J. Brazilian Soc. Mech. Sci. Eng. 39 (2017) 631–643. doi:10.1007/s40430-016-0569-8.

[28] M. Farzaneh-Gord, A. Arabkoohsar, M. Deymi Dasht-bayaz, V. Farzaneh-Kord, Feasibility of accompanying uncontrolled linear heater with solar system in natural gas pressure drop stations, Energy. 41 (2012) 420–428. doi:10.1016/j.energy.2012.02.058.

[29] A. Arabkoohsar, K.A.R. Ismail, L. Machado, R.N.N. Koury, Energy consumption minimization in an innovative hybrid power production station by employing PV and evacuated tube collector solar thermal systems, Renew. Energy. 93 (2016) 424–441. doi:https://doi.org/10.1016/j.renene.2016.03.003.

[30] http://sonda.ccst.inpe.br/basedados/saomartinho.html, (n.d.). http://sonda.ccst.inpe.br/basedados/saomartinho.html.

[31] R. Kemna, J. Acedo, Average EU building heat load for HVAC equipment, Final Rep. Framew. Contract ENER C. (2014). http://scholar.google.com/scholar?hl=en&btnG=Search&q=intitle:Average+EU+building+heat+load+for+HVAC+equipment#0.

[32] R. Lamberts, C. Candido, R. de Dear, R. De Vecchi, Towards a Brazilian Standard on Thermal Comfort, (2013) 123.

[33] M.D. Knudsen, S. Petersen, Model predictive control for demand response of domestic hot water preparation in ultra-low temperature district heating systems, Energy Build. 146 (2017) 55–64. doi:10.1016/j.enbuild.2017.04.023.

[34] F.J. Oppel, A.J. Ghajar, P.M. Moretti, Computer simulation of stratified heat storage, Appl. Energy. 23 (1986) 205–224. doi:https://doi.org/10.1016/0306-2619(86)90055-3.

- The concept of non-uniform temperature district heating is proposed and analyzed.
- The system works based on both ultralow- and medium-temperature modes every day.
- Neighborhood-scale storage tanks are used for domestic hot water demand coverage.
- The performance of the system is simulated and analyzed over an entire year.
- The system shows better efficiency and demand coverage compared to other schemes.